Hindawi
Journal of Chemistry
Volume 2019, Article ID 3547518, 10 pages
https://doi.org/10.1155/2019/3547518

Research Article

Effect of Dissolution and Dispersion Conditions of VC-713 on the Hydrate Inhibition

Ren Wang[1,2] **Huicui Sun**[3] **Jinsheng Sun**[1,2,4] **Yuanzhi Qu**[1,2] **Jie Zhang**[1,2] **Xiaomei Shi**[1] **Ling Zhang**[3] **and Dongdong Guo**[3]

[1]*CNPC Engineering Technology R & D Company Limited, Beijing 102206, China*
[2]*National Engineering Laboratory for Oil & Gas Drilling Technology, Beijing 102206, China*
[3]*Faculty of Engineering, China University of Geosciences, Wuhan 430074, Hubei, China*
[4]*Department of Petroleum Engineering, China University of Petroleum (East China), Qingdao 266580, Shandong, China*

Correspondence should be addressed to Jinsheng Sun; sunjsdri@cnpc.com.cn and Ling Zhang; ling.zhang@cug.edu.cn

Received 18 December 2018; Accepted 26 February 2019; Published 27 March 2019

Academic Editor: Woojin Lee

Copyright © 2019 Ren Wang et al. This is an open access article distributed under the Creative Commons Attribution License, which permits unrestricted use, distribution, and reproduction in any medium, provided the original work is properly cited.

VC-713 is a kind of hydrate kinetics inhibitor, which is widely used because of its strong hydrate inhibition. In this paper, VC-713 was dissolved and dispersed into its solution to various degrees by stirring the solution at the speeds of 600 r·min^{-1} and 12000 r·min^{-1}. Then, under the condition of normal pressure and temperature change (gradually decreasing from 278.15 K to 273.65 K), the hydrate inhibitory effect of dissolution and dispersion of VC-713 on THF hydrate formation was studied. The variation in the concentration of VC-713 was monitored during the experiments. In addition, the mesoscopic structure characteristics of aqueous solutions were observed, and experimental phenomena in the reactor were recorded along with real time. Then, the experimental data were comprehensively analyzed, and the underlying mechanism of inhibition was revealed. Results showed that VC-713 inhibits hydrate nucleation and growth by adsorbing and binding. When the addition amounts are the same, better dissolution and dispersion of VC-713 can inhibit the hydrate formation more effectively. This is due to more complex skeleton structures formed by the hydrated VC-713 molecule. When the amount of VC-713 is 0.5 wt.%, the induction time, the formation rate, and the degree of supercooling of hydrate formation were extended, mitigated, and increased by 10.30%, 21.43%, and 17.80%, respectively, and changed to values of 8.75%, 14.29%, and 22.50%, respectively, for 1.0 wt.% VC-713.

1. Introduction

As a clean alternative energy with great potential, natural gas hydrate has become a hot spot of academia, government, and various enterprises [1, 2]. However, in industrial production, the formation of hydrates may bring serious harm consequences. For example, when untreated oil and gas reservoirs transported through oil and gas pipelines contain natural gas and water, hydrates can be formed and aggregated at turns, reducers, valves, tee joints, separators, and other locations of the pipelines under appropriate temperature and pressure conditions, which will affect the safe transport of oil and gas [3–5]. During the construction of deep-sea conventional oil-and-gas drillings, shallow gas and hydrate decomposition gas will invade the drilling fluid and hydrates may be formed and aggregated in the annulus, and they will deteriorate the performance of drilling fluid and the efficiency of overall production [5–8]. During the exploiting of the sea area hydrates, the produced gas may form hydrates again at positions, such as wellbore gas-liquid separator and sand control liner, which will seriously affect the gas production efficiency [5, 9, 10]. When exploiting the sea area hydrates, the produced gas may form hydrates again at positions, such as wellbore gas-liquid separator and sand control liner, which seriously affect the gas production efficiency [5, 9, 10].

Thermodynamic inhibitors are widely used in the modern oil and gas industry to achieve complete suppression of the hydrate formation by changing their phase equilibrium conditions. However, thermodynamic inhibitors have certain

disadvantages, such as requirement of large quantities, high cost, and severe pollution. Therefore, researchers worldwide have focused on the development of environment-friendly kinetic inhibitors with less addition amount [11]. Most hydrate kinetic inhibitors are water-soluble molecular polymers, among which lactam polymers, amide polymers, and natural green polymers have been extensively studied [12]. Among them, the inhibitory effect of trimer inhibitor Gaffix VC-713 polymer (a terpolymer of vinyl caprolactam/vinylpyrrolidone/dimethylaminoethyl methacrylate, herein expressed as VC-713) on hydrate formation is superior to dimeric and monomeric inhibitors (under the same experimental conditions, the ability of VC-713 to inhibit the nucleation and growth of CH_4 hydrate is 3.5 times higher than that of PVPK90 [13]), and VC-713 is a more mature and widely used hydrate kinetic inhibitor [11, 12, 14]. It has been found that the mechanism of VC-713 inhibiting the hydrate formation may be similar to polyvinylpyrrolidone (PVP) [15–17]. That is, they adsorb the cage structure formed by the uncaged water molecules to prevent the guest molecules from entering the cage structure and thus suppressing the nucleation of hydrates [18, 19]. Furthermore, they adsorb and bind to the surface of the hydrate crystal particles to avoid the contact of guest and water molecules, and thereby inhibiting the growth of hydrates [20].

According to the abovementioned mechanism, it can be speculated that the dissolution and dispersion of VC-713 in the solution determines the size of its hydrated molecular aggregates and the tensile strength during the migration of aggregates (the resistance needed to overcome when the aggregates are broken and separated) [21, 22]. Consequently, it is likely to have an impact on its ability to inhibit hydrate formation. In order to verify this corollary and clarify the underlying mechanism of VC-713 inhibiting hydrate formation, different amounts of VC-713 (0.5 wt.% and 1.0 wt.%) were dissolved and dispersed in aqueous solutions to different degrees, and then, their hydrate inhibition was evaluated through tetrahydrofuran (THF) hydrate formation experiments (THF hydrate has been widely used for screening natural gas hydrate inhibitors because THF is a liquid entirely miscible with water and forms hydrate with water at 278.15 K and atmospheric pressure [23, 24]). According to the concentration change of VC-713 in the hydrate formation process and the mesoscopic structure of VC-713 aqueous solution, the impact mechanism is analyzed from macroscopic, mesoscopic, and microscopic scales. The obtained results are of important reference value to the development and industrial applications of hydrate kinetic inhibitors.

2. Experimental

2.1. Materials and Instruments. The materials used in the experiments included VC-713 obtained from International Special Products (ISP) Co., Ltd., USA; tetrahydrofuran (herein expressed as THF) obtained from Sinopharm Chemical Reagent Co., Ltd., China; and ultrapure water (herein expressed as UPW) with a resistivity of more than 18.25 M Ω cm, which was produced using a type UPW-S Millipore unit.

THF hydrate formation experiments were performed using a custom-made experimental setup (see Figure 1), which consisted of a temperature sensor with the accuracy of ±0.1 K and data acquisition frequency of once every 3 seconds. There is a sampling hole of 1.0 cm diameter in the sealing cover of metal reaction kettle. During the experiment, a sampling cylinder with a sieve (the diameter of the mesh was about 100 μm and the mesh was used to avoid the removal of hydrate during sampling) was used for liquid sampling work from the reaction vessel. The absorbance of the sample was measured using a Shimadzu UV-1800 UV-Visible spectrophotometer (experimental wavelength range: 190–1100 nm), from which the change in concentration of VC-713 in the sample was determined. In order to conduct mesostructure observations, initially the lyophilized samples from solutions were prepared using the Four-Ring LGJ-10D freeze dryer. Then, the samples were observed using a Phenom Pro desktop scanning electron microscope (SEM).

2.2. Methodology

2.2.1. Experiments on THF Hydrate Formation. In order to investigate the effect of dissolution and dispersion of VC-713 in solution on its hydrate inhibition, experiments were carried out on the formation of THF hydrates under the conditions of atmospheric pressure and different temperatures (each experiment was repeated thrice to ensure repeatability). The aqueous solutions of VC-713 with the concentrations of 0.5 wt.% and 1.0 wt.% were prepared under shearing rates of 600 r·min^{-1} and 12000 r·min^{-1}, respectively. The mass of the liquid sample to be tested in each experiment was 500 g (about 510 mL). The mass ratio of THF to UPW was 19 : 81 (under ideal conditions, all the solution could form THF hydrates [25]). The experimental procedure was as follows:

(1) A certain amount of the aqueous solution of VC-713 was prepared at the stirring speed of 600 r·min^{-1} and the stirring time of 2.0 h. In order to better dissolve and disperse VC-713 in the system, a certain amount of VC-713 aqueous solution was stirred for 30.0 min at the stirring speed of 12000 r·min^{-1} using a high-speed stirring device.

(2) The aqueous solution of VC-713 was injected into the reactor, and the temperature-control device, the temperature-monitoring system, and the mechanical stirring device were turned on. After the solution temperature reduced to 278.15 K and stabilized at this temperature under a dynamic stirring speed of 300 r·min^{-1}, THF was injected and the solution temperature was maintained at 278.15 K (THF hydrate cannot be formed under the condition of atmospheric pressure at this temperature [26]).

(3) The solution temperature was gradually reduced to 273.65 K by adjusting the temperature-control device, and the stirring speed of mechanical stirring

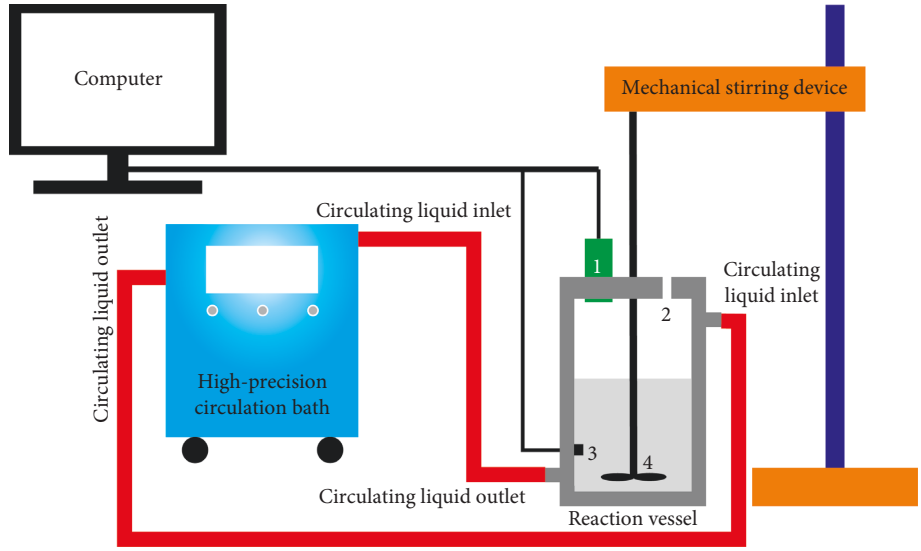

Figure 1: Schematic of the experimental setup.

device was reduced to 150 r·min^{-1}. Meanwhile, the high-definition camera was turned on to real-time recording of the experimental phenomenon inside the reactor.

2.2.2. Monitoring the Change in Concentration of VC-713. If the mechanism of VC-713 inhibiting the hydrate growth was the same as that of the PVP (which means further contact of guest and water molecules was prevented by binding the surface of the hydrate crystal particles, thereby inhibiting the growth of hydrate) [16, 17], the concentration of VC-713 in the solution would inevitably decrease with the increase of formed hydrate [27]. Therefore, in this work, from the hydrate being formed in each experiment, the liquid sample in the reactor was collected once every 20.0 min. Then, the UV-Visible spectrophotometer was used to monitor the absorbance of VC-713 in the sample, and the changes in concentration of VC-713 in the solution were monitored. The total number of samples for each experiment was 6, and each sample was ~7.0 mL in volume (it can be used for one test, while the UPW + THF system was also sampled following the same method to ensure that the experiments were under the same condition).

2.2.3. Observing the Mesoscopic Structure. It does great help in revealing the underlying mechanism of hydrate formation under different dissolution and dispersion conditions and at various concentrations to understand the mesostructural features of VC-713's aqueous solution [21]. Therefore, in this paper, the sample of each solution was first prepared by freeze-drying, and then SEM was used to observe the mesoscopic structure. The experimental procedure was as follows:

(1) A small amount of solution was taken using a dropper, dropped onto a mica film, and followed by placing it in liquid nitrogen for 2.0 min

(2) The frozen sample was then placed into a freeze-drier and lyophilized for 20.0 h

(3) SEM was used to observe the mesostructure after the sample preparation

3. Results

3.1. Evaluation of the Hydrate Inhibition. Figure 2 shows the variations of each experiment in temperature (take the curves obtained in one experiment as an example). The experimental data (see Table 1), such as the induction time of THF hydrate formation (determined through the generalized method [28]), and the supercooling condition (kinetic inhibitors do not change the hydrate phase equilibrium condition [15, 29, 30], whereas the phase equilibrium temperature for the formation of THF hydrate under atmospheric pressure is about 277.15 K [24, 26]) were obtained from Figure 2. From Figure 2 and the data in Table 1, it can be observed that, when the dissolution and dispersion condition of VC-713 in the sample was better and its concentration increased, the induction time of hydrate formation prolonged. Meanwhile, the supercooling degree of hydrate formation increased, and the increasing amplitude of temperature caused by the heat induced by hydrate formation was also diminished.

Since the time of complete formation of hydrate (based on Figure 2) cannot be accurately determined, the relevant experimental parameters need to be obtained through the real-time video data of the reactor. Figure 3 is the recording of the experimental process in the reactor for each

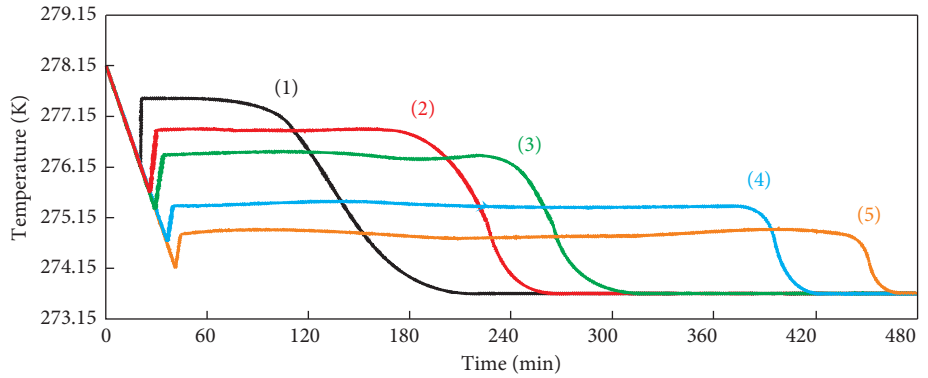

Figure 2: Variations in temperature with time for each experiment. (1) UPW + THF, (2) UPW + THF + 0.5 wt.% VC-713 (600 r·min^{-1}), (3) UPW + THF + 0.5 wt.% VC-713 (12000 r·min^{-1}), (4) UPW + THF + 1.0 wt.% VC-713 (600 r·min^{-1}), and (5) UPW + THF + 1.0 wt.% VC-713 (12000 r·min^{-1}). Initial temperature: 278.15 K.

Table 1: Experimental data for each experiment.

Samples	Induction time (min)	Undercooling (K)
UPW + THF	20.00 ± 1.20	274.55 ± 0.15
UPW + THF + 0.5 wt.% (600 r·min^{-1})	26.51 ± 0.52	275.06 ± 0.12
UPW + THF + 0.5 wt.% (12000 r·min^{-1})	29.24 ± 1.58	275.40 ± 0.23
UPW + THF + 1.0 wt.% (600 r·min^{-1})	38.16 ± 1.07	275.95 ± 0.17
UPW + THF + 1.0 wt.% (12000 r·min^{-1})	41.50 ± 2.35	276.58 ± 0.10

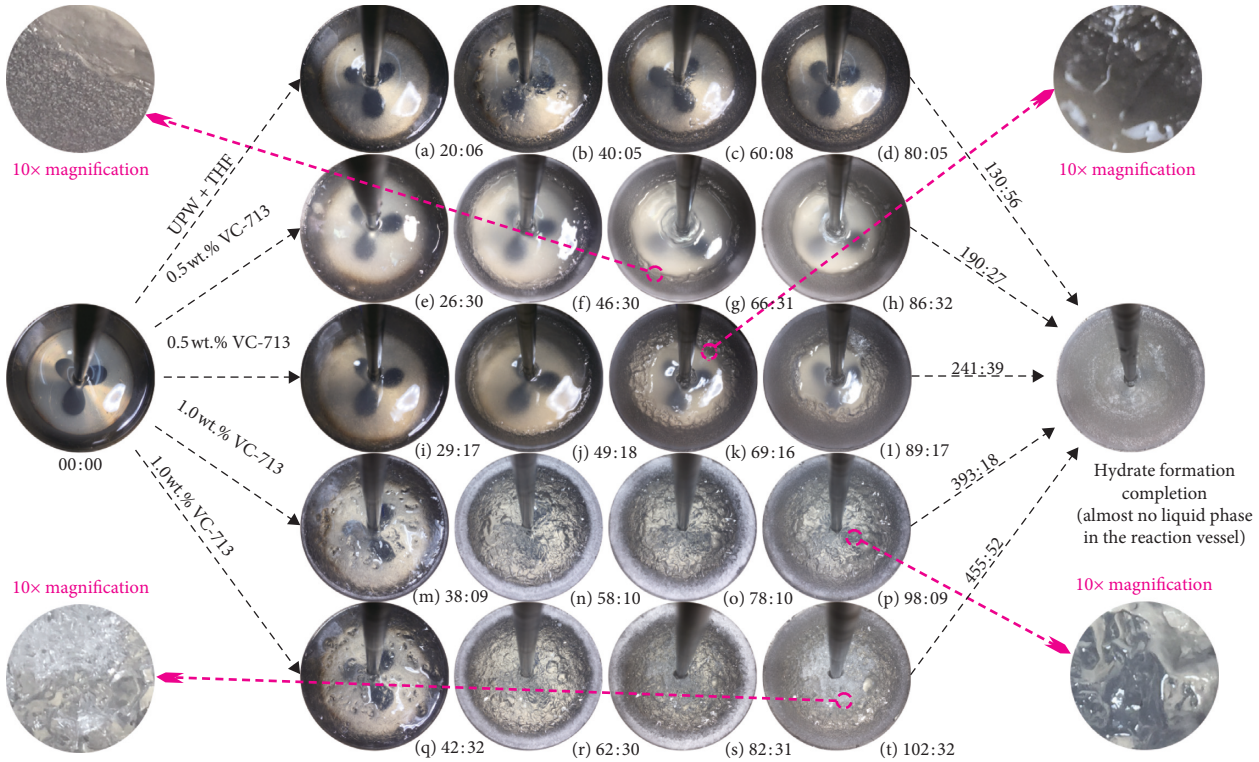

Figure 3: Photos of the progression of reaction inside the reactor at various time intervals. (a–d) UPW + THF; (c–h) UPW + THF + 0.5 wt.% VC-713 (600 r·min^{-1}); (i–l) UPW + THF + 0.5 wt.% VC-713 (12000 r·min^{-1}); (m–p) UPW + THF + 1.0 wt.% VC-713 (600 r·min^{-1}); (q–t) UPW + THF + 1.0 wt.% VC-713 (12000 r·min^{-1}).

experiment. It is well known that the liquid sample tested for each experiment will eventually form THF hydrates, and thus, the amount of hydrate formation can be characterized based upon the mass of THF involved in the reaction. The average rate of hydrate formation can be calculated using the following equation.

$$v = \frac{\Delta n}{t}, \quad (1)$$

where v is the average consumption rate of THF, g min^{-1}; Δn is the consumption of THF, g; and t is the time elapsed from the beginning to the end of hydrate formation, min.

Since the sampling times and the amounts of liquid samples were the same for all experiments, it can be shown that the THF mass involved in the hydrate formation for each group (of experiments) was ~53.82 g (calculated based on the solution mass and the volume ratio). In addition, t was obtained from Figure 3, while the v values (from top to bottom in Table 1) for the experiments were calculated as 0.41 g min^{-1}, 0.28 g min^{-1}, 0.22 g min^{-1}, 0.14 g min^{-1}, and 0.12 g min^{-1}, respectively.

It can be concluded that, when the added amount of VC-713 was 0.5 wt.%, the induction time of the hydrate formation in the solution prepared using high-speed stirring was 10.30% longer than that prepared using low-speed stirring. Hydrate formation rate decreased by 21.43% and the undercooling of hydrate nucleation increased by 17.80%. When the addition amount of VC-713 was 1.0 wt.%, compared with the solution prepared using low-speed stirring, the induction time of the hydrate formation prolonged by 8.75%, while the hydrate formation rate reduced by 14.29%. Additionally, the undercooling of hydrate nucleation increased by 22.50% with the increase of the formulated solution stirring rate. Furthermore, the ability of VC-713 in inhibiting the nucleation and growth of hydrate enhanced as the increase of the addition amount of VC-713 under the same stirring rate (there was a large difference between the experimental result and that obtained from Lederhos et al. [15]).

3.2. Change in the Concentration of VC-713. In this experiment, the concentration of VC-713 in each solution was calculated using the following equation [31].

$$A = \varepsilon \cdot c \cdot l, \quad (2)$$

where A is the absorbance (measured directly); ε is the absorption coefficient, L mol^{-1} cm^{-1}; c is the concentration of the substance to be tested, mol L^{-1}; and l is the solution thickness (measured directly), cm. The initial concentration of VC-713 (c value) for each solution was known, and the values of A and l (A value peaked at $l = 227$ nm) could be obtained from the base test sample (UPW + VC-713). Then, the specific ε value of VC-713 could be calculated using equation (2). Based upon the value of ε, the concentrations of VC-713 in the samples at different time intervals were calculated. The experimental results are shown in Figure 4.

As can be seen from Figure 4, the VC-713 concentration in the solution (that was not involved in the hydrate formation) gradually decreased with the formation of THF hydrates in each experiment. However, for the solution prepared using high-speed stirring, the decreasing rate of the concentration of VC-713 was relatively low, and the amplitude of drop was relatively smaller.

3.3. Mesoscopic Structural Characteristics of the Solution. The mesostructures of the freeze-dried samples for the experiments are shown in Figure 5. Among them, the greyish white parts were hydrated VC-713 molecular aggregates, while the dark parts were porous spaces. It can be found from Figure 4 that, for VC-713 in the formulated solutions at different concentrations and stirring speeds, its hydrated molecules aggregated to form smooth sheet-like and thin rod-shaped skeletons with different sizes and densities. Therefore, they constituted the network skeleton structures with different spatial forms. Hydrated VC-713 molecular aggregates mainly existed in the form of smooth flaky skeleton (~10–40 μm in diameter and ~0.2–0.5 μm in thickness) in the solution prepared using the low-speed stirring at a concentration of 0.5 wt.%. In addition, a small amount of thin rod-shaped skeleton (~0.5–1.5 μm in diameter) was also observed, which led to the presence of more porous spaces having larger size (~10–80 μm in diameter) between the network skeletons. The network structure of hydrated VC-713 molecular aggregates changed obviously with the increase of the formulated solution stirring rates under the same solution concentration. Meanwhile, hydrated VC-713 molecular aggregates mainly existed in the form of thin rod-like skeleton (~0.5–1.0 μm in diameter). The number of sheet-like skeletons greatly reduced, and the size was significantly reduced (~2–20 μm in diameter and ~0.2 μm in thickness). The network skeleton structure became more complex and the diameter of the porous space reduced to 2–10 μm, indicating that the stirring and shearing action at high speed promoted better dissolution and dispersion of VC-713 in the system.

Hydrated VC-713 molecular aggregates also existed mainly in the form of smooth flaky skeleton (similar to the solution concentration of 0.5 wt.%) in a 1.0 wt.% solution prepared using low-speed stirring. However, the area (~40–100 μm in diameter) and the thickness (~0.2–1.0 μm) both increased. Although the amount of thin rod-like skeleton was smaller in diameter (~1.0–2.0 μm), the porous space became much smaller in diameter (~5–60 μm). Moreover, there were very thin and porous hydrated molecular aggregates between the flaky skeletons, which played a supporting role and thus created the network skeleton morphology more complex. When the stirring speed of the solution was increased to 12000 r·min^{-1}, VC-713, with the amount of 1.0 wt.%, can also be better dissolved and dispersed in the system. In this case, the size of the sheet-like skeleton (~20–60 μm in diameter and ~0.2–0.5 μm in thickness) was reduced, and the number of thin rod-like skeletons increased (~0.5–1.0 μm in diameter). Furthermore, very thin and porous hydrated molecular aggregates were densely distributed among the flaky skeletons, thus making the network skeleton structure more complex and the size of porous space relatively smaller (~1–5 μm in diameter).

In summary, the high-speed stirring and shearing effect promoted the dissolution and dispersion of VC-713 in the system, reduced the size of hydrated VC-713 molecular aggregates, increased the specific surface area of the aggregates, created a more complex network skeleton structure, and reduced the porous space size among the skeleton

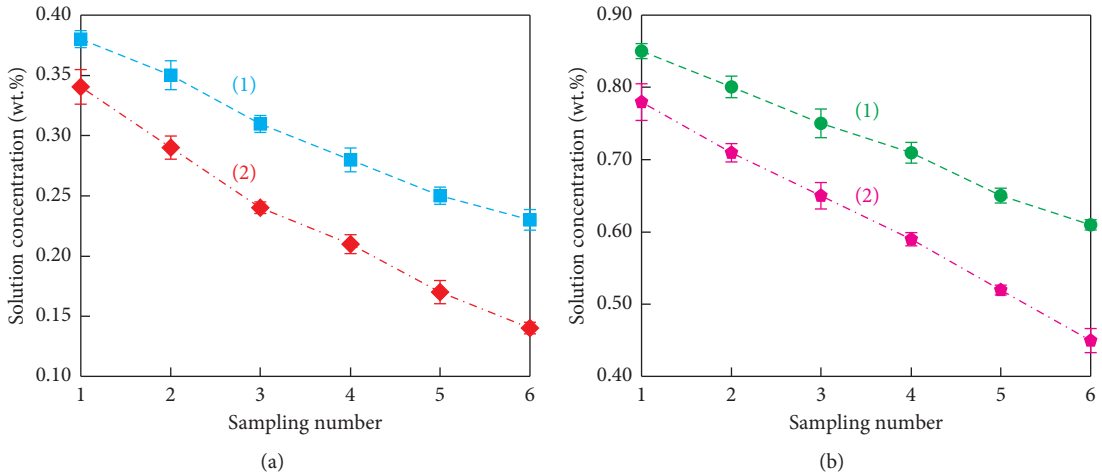

Figure 4: Changes in the concentration of VC-713 with the growth of hydrates in each experiment. (a-1) UPW + THF + 0.5 wt.% VC-713 (600 r·min^{-1}); (a-2) UPW + THF + 0.5 wt.% VC-713 (12000 r·min^{-1}); (b-1) UPW + THF + 1.0 wt.% VC-713 (600 r·min^{-1}); (b-2) UPW + THF + 1.0 wt.% VC-713 (12000 r·min^{-1}).

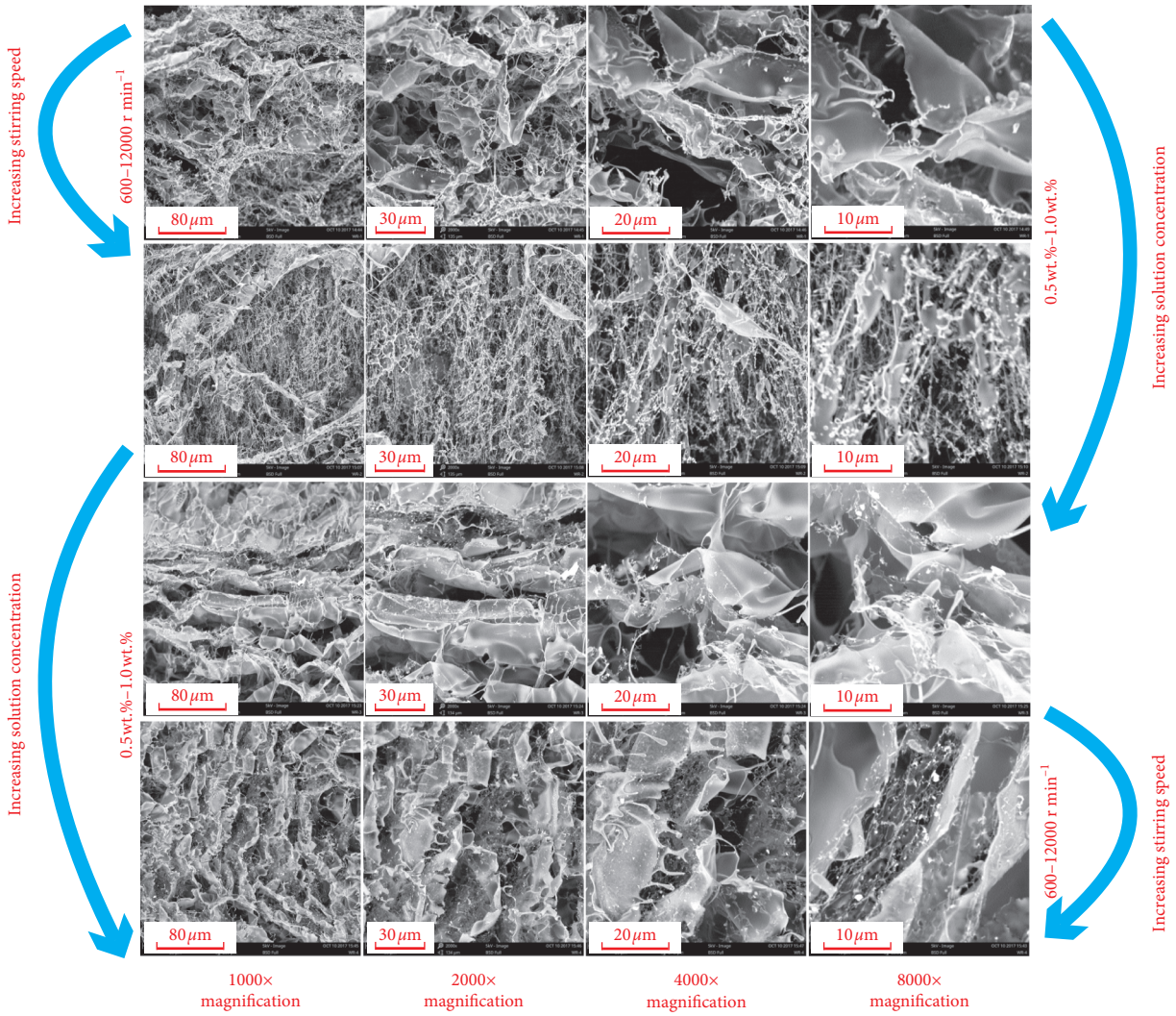

Figure 5: Mesostructure of each aqueous solution.

structures. Increasing the added amount of VC-713 to the system also made the network skeleton structure (composed of hydrated molecules) more complex and the size of the porous space among the network frameworks smaller due to the increase in the size of hydrated VC-713 molecular aggregates. These changes and differences were most likely to influence and determine the hydrate inhibition of each solution [21].

4. Analysis and Discussion

From the above results, it can be concluded that, with the same added amount of VC-713 to the solution, high-speed stirring of the solution could result in better dissolution and dispersion of VC-713 in the system, and therefore, enhance the hydrate inhibition of VC-713 to some extent. This was evidently displayed by the extension of the induction time of THF hydrate formation. The rate of hydrate formation was also slowed down and the undercooling of hydrate nucleation was increased. The extended induction time and the increase of undercooling indicated that VC-713 with better dissolution and dispersion was more effective in inhibiting the hydrate nucleation. When the water molecules in the system were aligned to form an unclosed cage structure (driven by hydration), VC-713 will adsorb on the surface of the cage structure under the influence of its own lactam ring to prevent the guest molecules from entering the cage, thus inhibiting the nucleation of the hydrates. As shown in Figure 5, VC-713 in the solution existed in the form of hydrated molecular aggregates, whereas the porous space of the formed skeleton structure was filled with UPW and THF. Under different dissolution and dispersion conditions with the same added amount of VC-713 in the system, the smaller the sizes of the hydrated molecular aggregates were, the more complex the skeleton structure was and the smaller the porous space among the skeleton structures was. During the formation of the cage structure of the water molecules, when the tensile strength of the framework structure was relatively small (high-speed stirring and shearing will reduce the tensile strength of VC-713 hydrated molecular aggregates [22]), VC-713 was more susceptible to fracturing, peeling off, and migration to the surface of the unoccupied cage structure. Moreover, the migration distance of VC-713 was relatively short owing to the small porous space size of the skeleton structure, which reduced the migration time. Therefore, VC-713 could better suppress the nucleation of hydrates.

It is known that VC-713 showed certain adsorption properties to hydrophilic hydrate crystal particles under the influence of its own lactam ring and exhibited a film-forming character [17]. These would prompt VC-713 to adsorb the surface of the hydrate crystal particles, whereas the hydrate crystal particles will be completely bound by VC-713, thereby inhibiting the growth of hydrates. In order to verify this hypothesis, the changes in concentration of VC-713 in the solution (which did not participate in the hydrate formation process) were monitored during each experiment. The results showed that, with the increase of the THF hydrate formation amount, the concentrations of VC-713 in the solutions gradually decreased (see Figure 4). This indicated that the hydrate formation consumed a certain amount of VC-713, which was caused by the adsorption and encapsulation of hydrates by VC-713 (similar to the hydrate growth inhibiting mechanism of PVP [27]). The study results proved the aforementioned speculations and clearly identified the kinetic mechanism of VC-713 for inhibiting hydrates growth.

It is noteworthy that when the dissolution and dispersion of VC-713 in the system were relatively better, the rate of hydrate formation was relatively lower, indicating the enhanced ability of VC-713 for inhibiting the growth of hydrates. Figure 4 shows that, under better dissolution and dispersion conditions and for the same added amount of VC-713, the rate of consumption of VC-713 was relatively slower during the formation of hydrates. The relatively higher concentration of VC-713 in the solution facilitated the inhibition of further hydrate growth, which was not involved in the formation of hydrates. The better dissolution and dispersion conditions of VC-713 led to its much slower consumption rate in the process of hydrate growth, which was probably related to the sizes of the aggregates formed by its hydrated molecules in the solution. As shown in Figure 5, after the formation of hydrates in the void space of the VC-713 skeleton structure, the hydrated VC-713 molecular aggregates with small sizes, which had relatively small size and were susceptible to fracture and peel off, could move to the vicinity of the aggregates of the crystal particles more easily and rapidly, thus inhibiting further growth of the hydrates by binding to the surface. Furthermore, due to the relatively large specific surface area of the hydrated molecular aggregates, a small amount of VC-713 could bind to the surface of the hydrate crystal particles or crystal particle aggregates (as shown in Figure 6), and thus reduce the amount (consumed) and the consumption rate of VC-713.

By observing the magnified images of THF hydrate morphology in Figures 3(f) and 3(j), it can be found that the skeleton structure composed of the hydrated molecules was more complex when the dissolution and dispersion of VC-713 were better. Although the fracture and peeling of skeleton structure were relatively easier, the formation of hydrates would consume a certain amount of VC-713, whereas the gas-liquid interface in the reactor would retain a certain amount of the grid-like aggregate system composed of unspoilt hydrates and VC-713 even under dynamic conditions (the underlying mechanism of this experimental phenomenon was likely to be the same as that shown in Figure 6). Figures 3(n)–3(p) and 3(r)–3(t) show that, when the added amount of VC-713 increased and the skeleton structure constituted by its hydration molecules was relatively stable, the reactor gas-liquid interface would form a more stable grid-shaped hydrates and VC-713 aggregation system with distinct morphological characteristics. By comparing Figures 3(p) and 3(t), it can be seen that, the smaller the pore space size in the skeleton structure composed of hydrated VC-713 molecules were, the smaller the size of the hydrate aggregates in the porous space was and the harder it was for the hydrate crystal particles to grow

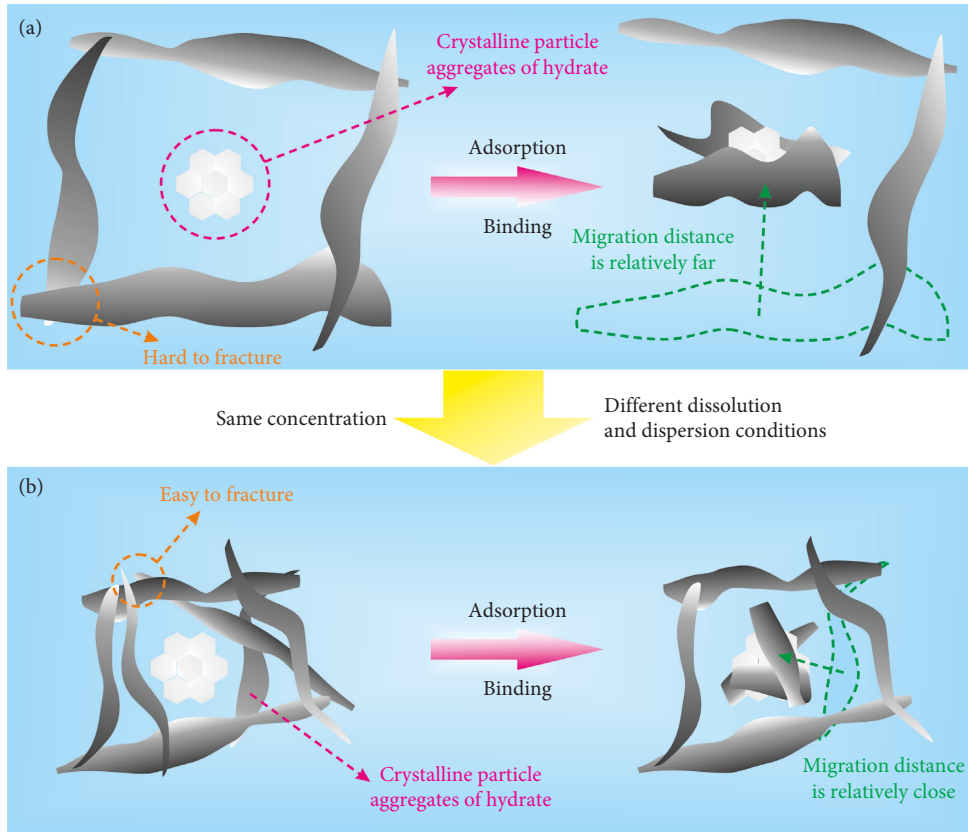

Figure 6: The possible inhibiting mechanism of hydrate growth by VC-713 with different degrees of dissolution and dispersion. (a) Stirring rate is 600 r·min^{-1}; (b) Stirring rate is 12000 r·min^{-1}.

and aggregate to form large aggregates. Therefore, the experimental phenomena presented in Figure 3 are more intuitive to verify the analytically obtained underlying mechanisms in this study.

Under the experimental conditions where the dissolution and dispersion conditions of VC-713 in the system were the same, the ability of VC-713 for inhibiting the nucleation and growth of hydrate was improved when the addition amount of VC-713 was increased from 0.5 wt.% to 1.0 wt.%. However, it is worth noticing that the hydrate kinetic inhibitors (such as PVP and polyvinylcaprolactam) do not show a stronger inhibiting ability with any higher addition amount [15, 32, 33]. Therefore, it seems that there is an optimum value of VC-713's addition amount. Below this value, the hydrate inhibition of VC-713 will be weakened, while above this threshold value, the hydrate inhibition of VC-713 may either no longer be enhanced or weakened, or the hydrate formation will be promoted. A comprehensive and in-depth study on the critical value of the addition amount of VC-713 will be conducted in the future study, which will aim to provide a more valuable reference for the industrial application of VC-713.

5. Conclusions

In this study, VC-713 was dissolved and dispersed in solution to different degrees using stirring speeds and shearing at 600 r min^{-1} and 12000 r min^{-1}. Under the dynamic conditions of the atmospheric pressure, variable temperature, and mechanical agitation, based on the parameters of induction time, average formation rate, and undercooling of THF hydrate formation in UPW + THF system, the effects of dissolution and dispersion conditions of VC-713 on its hydrate inhibition were investigated from macroscopic, mesoscopic, and microscopic levels combining with the experimental methods of the monitoring of the change in the concentration of VC-713 during hydrate formation, the mesoscopic structure of the solution, and the real-time recording of the experimental phenomena. Although the mechanism analysis of VC-713 to inhibit the nucleation of hydrates was still based on existing research results, the underlying mechanism of VC-713 for inhibiting the growth of hydrates was clarified through experiments, and the changes in its hydrate inhibition were also analyzed and compared with the added mount of VC-713 from 0.5 wt% to 1.0 wt%. Based upon the results, the following conclusions are drawn:

(1) VC-713 with better dissolution and dispersion conditions in the system can inhibit the nucleation and growth of hydrates more effectively when the addition amount of VC-713 is same. When the addition amount was 0.5 wt.%, the induction time of the hydrate formation was prolonged by 10.30%, while the formation rate was slowed down by

21.43%. Additionally, the undercooling of hydrate formation was increased by 17.80%. When the addition amount was 1.0 wt.%, the inducing time, rate, and the undercooling of hydrate formation were prolonged, slowed down, and increased by 8.75%, 14.29%, and 22.50%, respectively.

(2) Influenced by its own lactam rings and film-forming property, the VC-713 inhibited the nucleation and growth of the hydrates through adsorption and binding. Under different dissolution and dispersion conditions of VC-713 in the system, the spatial morphology of the network skeleton composed of hydrated molecular aggregates and the difficulty of fracture and peeling of the skeleton became different. These differences determined the inhibition ability of the system for hydrate formation in space and time.

(3) The hydrate inhibition of VC-173 is enhanced as its added amount increased from 0.5 wt.% to 1.0 wt.% under the same dissolution and dispersion conditions. However, the addition amount of VC-713 is likely to have a threshold (optimum) value for the inhibition of hydrates. Therefore, 1.0 wt.% of VC-713 may not be the optimum added amount.

Data Availability

The data used to support the findings of this study are included within the article. All data included in this study are available from the corresponding author upon request.

Conflicts of Interest

The authors declare that they have no conflicts of interest.

Acknowledgments

This work was supported by the Research Project of CNPC Engineering Technology R & D Company limited (CPET201807), the National Natural Science Foundation of China (51874263), and the Qingdao City: Program for Entrepreneurial and Innovative Leading Talents (No. 18-1-2-15-zhc).

References

[1] E. D. Sloan, "Fundamental principles and applications of natural gas hydrates," *Nature*, vol. 426, no. 6964, pp. 353–359, 2003.

[2] E. D. Sloan, "Introductory overview: hydrate knowledge development," *American Mineralogist*, vol. 89, no. 8-9, pp. 1155–1161, 2004.

[3] M. N. Lingelem, A. I. Majeed, and E. Stange, "Industrial experience in evaluation of hydrate formation, inhibition, and dissociation in pipeline design and operation," *Annals of the New York Academy of Sciences*, vol. 715, no. 1, pp. 75–93, 1994.

[4] A. K. Sum, C. A. Koh, and E. D. Sloan, "Clathrate hydrates: from laboratory science to engineering practice," *Industrial & Engineering Chemistry Research*, vol. 48, no. 16, pp. 7457–7465, 2009.

[5] R. Wang, F. L. Ning, T. L. Liu et al., "Dynamic simulation of hydrate formed from free methane gas in borehole," *Acta Petrologica Sinica*, vol. 38, pp. 963–972, 2017.

[6] F. Ning, L. Zhang, Y. Tu, G. Jiang, and M. Shi, "Gas-hydrate formation, agglomeration and inhibition in oil-based drilling fluids for deep-water drilling," *Journal of Natural Gas Chemistry*, vol. 19, no. 3, pp. 234–240, 2010.

[7] D. R. McConnell, Z. Zhang, and R. Boswell, "Review of progress in evaluating gas hydrate drilling hazards," *Marine and Petroleum Geology*, vol. 34, no. 1, pp. 209–223, 2012.

[8] R. Wang, T. L. Liu, F. L. Ning et al., "Effect of hydrophilic silica nanoparticles on hydrate formation: insight from the experimental study," *Journal of Energy Chemistry*, vol. 30, pp. 90–100, 2019.

[9] E. D. Sloan, "A changing hydrate paradigm-from apprehension to avoidance to risk management," *Fluid Phase Equilibria*, vol. 228-229, pp. 67–74, 2005.

[10] X. K. Ruan, X. S. Li, M. J. Yang, and F. Yu, "Influences of gas hydrate reformation and permeability changes on depressurization recovery," *Acta Petrologica Sinica*, vol. 36, pp. 612–619, 2015.

[11] S. S. Fan, Y. H. Wang, and X. M. Lang, "Progress in the research of kinetic hydrate inhibitors," *Natural Gas Industry*, vol. 31, pp. 99–109, 2011.

[12] M. S. Kamal, I. A. Hussein, A. S. Sultan, and N. von Solms, "Application of various water soluble polymers in gas hydrate inhibition," *Renewable and Sustainable Energy Reviews*, vol. 60, pp. 206–225, 2016.

[13] T. He, "*Synthesis and evaluation of natural gas hydrate kinetic inhibitors*," M.S. thesis, Southwest Petroleum University, Chengdu, China, 2017.

[14] H. Sharifi, J. Ripmeester, V. K. Walker, and P. Englezos, "Kinetic inhibition of natural gas hydrates in saline solutions and heptane," *Fuel*, vol. 117, pp. 109–117, 2014.

[15] J. P. Lederhos, J. P. Long, A. Sum, R. L. Christiansen, and E. D. Sloan, "Effective kinetic inhibitors for natural gas hydrates," *Chemical Engineering Science*, vol. 51, no. 8, pp. 1221–1229, 1996.

[16] C. A. Koh, R. E. Westacott, W. Zhang, K. Hirachand, J. L. Creek, and A. K. Soper, "Mechanisms of gas hydrate formation and inhibition," *Fluid Phase Equilibria*, vol. 194–197, pp. 143–151, 2002.

[17] B.-Z. Peng, C.-Y. Sun, P. Liu, Y.-T. Liu, J. Chen, and G.-J. Chen, "Interfacial properties of methane/aqueous VC-713 solution under hydrate formation conditions," *Journal of Colloid and Interface Science*, vol. 336, no. 2, pp. 738–742, 2009.

[18] T. J. Carver, M. G. B. Drew, and P. M. Rodger, "Inhibition of crystal growth in methane hydrate," *Journal of the Chemical Society, Faraday Transactions*, vol. 91, no. 19, pp. 3449–3460, 1995.

[19] H. Ohno, I. Moudrakovski, R. Gordienko, J. Ripmeester, and V. K. Walker, "Structures of hydrocarbon hydrates during formation with and without inhibitors," *Journal of Physical Chemistry A*, vol. 116, no. 5, pp. 1337–1343, 2012.

[20] H. Zeng, H. Lu, E. Huva, V. K. Walker, and J. A. Ripmeester, "Differences in nucleator adsorption may explain distinct inhibition activities of two gas hydrate kinetic inhibitors," *Chemical Engineering Science*, vol. 63, no. 15, pp. 4026–4029, 2008.

[21] L. Zhang, H. Sun, B. Han et al., "Effect of shearing actions on the rheological properties and mesostructures of CMC, PVP and CMC+PVP aqueous solutions as simple water-based drilling fluids for gas hydrate drilling," *Journal of Unconventional Oil and Gas Resources*, vol. 14, pp. 86–98, 2016.

[22] X. X. Song, "*The research of mechanical viscosity loss of polymer injection allocation flooding in the near-well zone*," M.S. thesis, Harbin Institute of Technology, Harbin, China, 2016.

[23] W. C. Wang, Y. X. Li, S. S. Fan, and D. Q. Liang, "Flow behaviors of tetrahydrofuran hydrate slurry," *Chemical Industry and Engineering Progress*, vol. 29, pp. 1418–1422, 2010.

[24] P. Naeiji, A. Arjomandi, and F. Varaminian, "Amino acids as kinetic inhibitors for tetrahydrofuran hydrate formation: experimental study and kinetic modeling," *Journal of Natural Gas Science and Engineering*, vol. 21, pp. 64–70, 2014.

[25] H. Conrad, F. Lehmkühler, C. Sternemann et al., "Tetrahydrofuran clathrate hydrate formation," *Physical Review Letters*, vol. 103, no. 21, pp. 218–301, 2009.

[26] E. D. Sloan and C. A. Koh, *Clathrate Hydrates of Natural Gases*, CRC Press, Boca Raton, FL, USA, 3rd edition, 2008.

[27] J. Ivall, J. Pasieka, D. Posteraro, and P. Servio, "Profiling the concentration of the kinetic inhibitor polyvinylpyrrolidone throughout the methane hydrate formation process," *Energy and Fuels*, vol. 29, no. 4, pp. 2329–2335, 2015.

[28] P. Skovborg, H. J. Ng, P. Rasmussen, and U. Mohn, "Measurement of induction times for the formation of methane and ethane gas hydrates," *Chemical Engineering Science*, vol. 48, no. 3, pp. 445–453, 1993.

[29] P. K. Notz, S. Bumgartner, B. D. Schaneman, and J. L. Todd, "The application of kinetic inhibitors to gas hydrate problems," *SPE Production and Facilities*, vol. 11, no. 4, pp. 256–260, 1996.

[30] N. J. Phillips and M. Grainger, "Development and application of kinetic hydrate inhibitors in the North Sea," in *Proceedings of SPE Gas Technology Symposium*, p. 397, Calgary, Canada, March 1998.

[31] R. Chang, *Physical Chemistry for the Chemical and Biological Sciences*, University Science Books, Sausalito, CA, USA, 2000.

[32] A. Ding, S. Wang, T. Pelemis, C. Crisafio, and X. Lou, "Specific critical concentrations of low dosage hydrate inhibitors in a THF-NaCl hydrate formation solution," *Asia-Pacific Journal of Chemical Engineering*, vol. 5, no. 4, pp. 577–584, 2010.

[33] J. Y. Liu, J. Zhang, G. D. Zhang, W. H. Zhang, and J. Wei, "Evaluation and application of a new hydrate kinetic inhibitor," *Natural Gas Industry*, vol. 31, pp. 65–68, 2011.

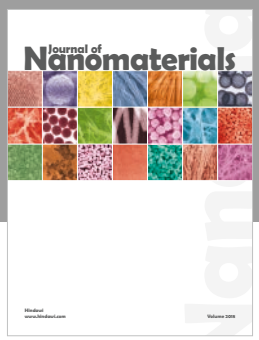

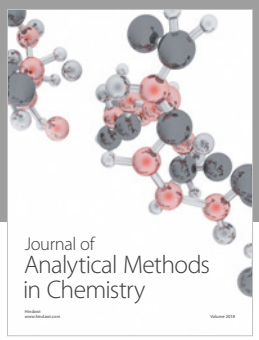

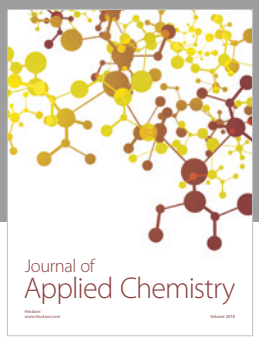

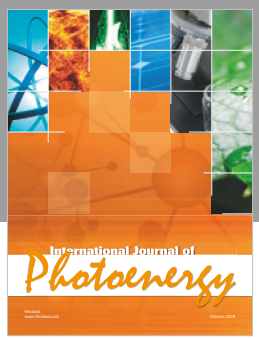

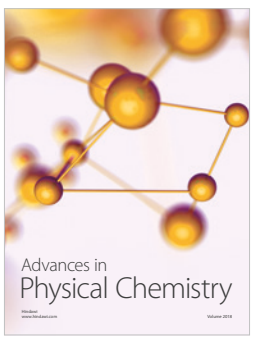

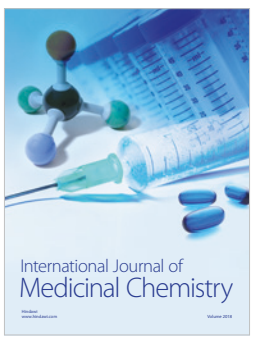

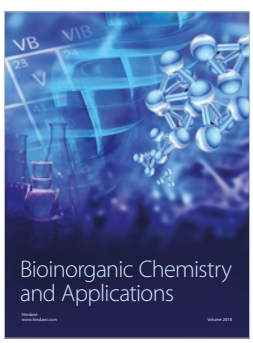

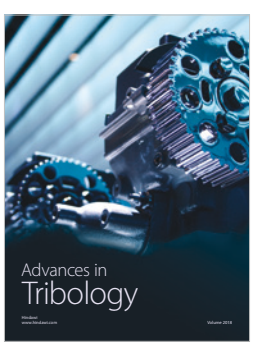

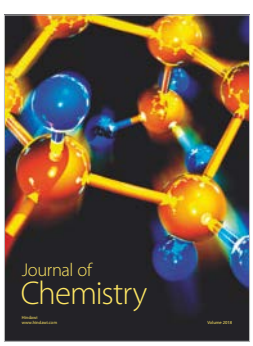

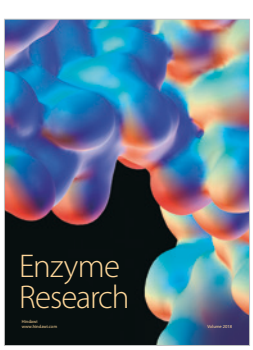

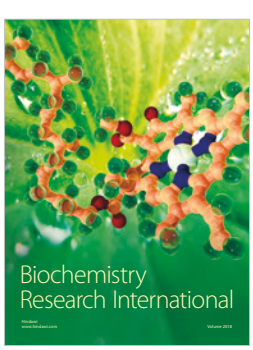

Hindawi

Submit your manuscripts at
www.hindawi.com